

ARTICLES

An asteroid breakup 160 Myr ago as the probable source of the K/T impactor

William F. Bottke¹, David Vokrouhlický^{1,2} & David Nesvorný¹

The terrestrial and lunar cratering rate is often assumed to have been nearly constant over the past 3 Gyr. Different lines of evidence, however, suggest that the impact flux from kilometre-sized bodies increased by at least a factor of two over the long-term average during the past ~100 Myr. Here we argue that this apparent surge was triggered by the catastrophic disruption of the parent body of the asteroid Baptistina, which we infer was a ~170-km-diameter body (carbonaceous-chondrite-like) that broke up 160^{+30}_{-20} Myr ago in the inner main asteroid belt. Fragments produced by the collision were slowly delivered by dynamical processes to orbits where they could strike the terrestrial planets. We find that this asteroid shower is the most likely source (>90 per cent probability) of the Chicxulub impactor that produced the Cretaceous/Tertiary (K/T) mass extinction event 65 Myr ago.

The nature of the terrestrial and lunar impact flux over the past several Gyr has been subject to considerable debate, with key arguments focusing on the dominance of asteroidal versus cometary impactors and whether the flux is constant, cyclic, or is punctuated in some manner with random ‘showers’. Although all attempts to identify a cycle period in the impact crater data have largely failed, the issue of whether the impact flux has varied, and if so by how much, over what timescale, and by what mechanism, is nevertheless an important one for understanding the geological and biological history of our planet. The fact that the current population of near-Earth objects (NEOs) looks reasonably close to what would be expected from a constant background flux from the asteroid belt¹, and that the present-day impact flux from those bodies seems to match up, more or less, with the long-term average flux over billions of years^{2–4}, suggests that any putative showers must be either of very short duration or of modest increase over the background for a more prolonged period.

In this light, it is useful to examine the recent impact history of the Earth and Moon to see whether insights into these issues can be gleaned from the best preserved and most accessible craters. An analysis of terrestrial craters found on stable cratons in North America, Europe and Australia suggests the collision rate of diameter $D \geq 1$ km projectiles may have increased by a factor of ~2 or so over the past ~100 Myr (refs 3–6). Some even argue that the terrestrial crater record supports a fourfold increase over this time, though this has yet to be verified⁷. Studies of lunar craters also support a factor of 2 increase in the recent impact flux (for example, counts of craters found within $D > 8$ km craters on the lunar nearside⁸, counts of craters on/near the 109-Myr-old Tycho crater⁴, and estimates of the impact flux from lunar rayed craters⁵, although also see ref. 6). These data sets should be interpreted with some caution; we note that few craters on the Moon have well-determined ages. Still, a recent increase in the multi-kilometre impactor flux would provide the simplest way to explain the abundance of impact-derived glass spherules with relatively young ages found in lunar soils (see, for example, ref. 9).

In the past, it was assumed that sudden changes in the terrestrial planet impactor flux must come from comet showers, presumably produced by the passage of a star through the Oort cloud (see, for example, ref. 3). The expected duration of these showers, however, is only a few Myr (ref. 10), too short to explain the crater and impact-spherule age distributions described above. Moreover, our

current understanding of the active and dormant populations of Jupiter-family comets^{2,11} and nearly isotropic comets^{11,12} (see also Supplementary Discussion) suggests that these objects strike the Earth and Moon too infrequently to be considered a plausible source for any prolonged increase in the impact flux. The comet shower model has been further weakened by the fact that several large terrestrial craters once assumed to have been produced by comets³ have now been linked to projectiles with asteroid-like compositions^{13,14}.

We instead argue here that the increased impact flux described above was set off by the catastrophic disruption of a ~170-km body in the innermost region of the main asteroid belt. This breakup event produced what is now known as the Baptistina asteroid family (BAF), a cluster of fragments with similar proper semimajor axes a , eccentricities e and inclinations i . According to our numerical simulations, the BAF’s location, age and fragment size distribution are remarkably well suited to generate a ~100-Myr-long surge in the multi-kilometre NEO population and explain the above observations. Moreover, the bombardment created by the BAF provides the most probable source for the projectiles that produced the K/T impact on Earth and the conspicuous Tycho crater on the Moon. Interpreted more broadly, this event can be considered powerful evidence for a recurrent process in which the formation of inner main belt families like Flora or Vesta leads to showers of debris delivered to Earth^{15–17}.

Identifying the Baptistina family

The BAF is centred on (298) Baptistina, a $D \approx 40$ km asteroid with proper semimajor axis $a_{\text{bap}} = 2.26$ AU (ref. 18) and spectroscopic characteristics similar to carbonaceous chondrites (that is, those resembling C- or X-type asteroids)¹⁹ (see Supplementary Discussion). Figure 1 shows our best estimate of the observed BAF and also describes how it was identified. The family resides in a complicated region of the main belt; it is partially overlapped by the prominent Flora and Vesta families, and is nearly bisected by the 7:2 and 5:9 mean motion resonances with Jupiter and Mars, respectively²⁰ (we refer to these mean motion resonances together as the J7:2/M5:9).

To pick out BAF members from the background, we take advantage of recent advances in our knowledge of the dynamical evolution and spectroscopic properties of asteroid families. For the former, it is now recognized that small asteroids are affected by the Yarkovsky and YORP (Yarkovsky–O’Keefe–Radzievskii–Paddack) effects, thermal

¹Southwest Research Institute, 1050 Walnut St, Suite 300, Boulder, Colorado 80302, USA. ²Institute of Astronomy, Charles University, V Holešovičkách 2, 18000 Prague 8, Czech Republic.

radiation forces and torques that cause $D < 40$ km objects to undergo semimajor axis drift and spin vector modifications, respectively, as a function of their size, spin vector, orbit and physical/material properties²¹. These non-gravitational perturbations leave their mark on families, causing them to evolve in ways that produce characteristic fingerprints in orbital element space²² (see Supplementary Discussion).

Immediately after an asteroid breakup event, individual fragments begin to spread in semimajor axis a by the Yarkovsky effect, with smaller bodies drifting inward towards or outward away from the Sun faster than larger bodies²¹. At the same time, the YORP effect works to preferentially tilt the obliquities of the fragments towards 0° or 180° , values that optimize their da/dt drift rates. Numerical simulations show that over time, the coupled Yarkovsky/YORP effects cause a family to evolve into a two-lobed structure in a and absolute magnitude H space (a, H), with each lobe filled with fast-moving asteroids headed for the family's periphery²² (see Supplementary Discussion). This dynamical signature, which has already been identified in several young families²², is seen in Fig. 1. The dark grey lines show our estimate of the borders of the BAF. According to Yarkovsky/YORP evolution models, the BAF boundaries are defined as the outermost region of each lobe in (a, H) space where the number density of asteroids is significantly higher than in the background. Objects outside the lines should mostly be background objects (see Supplementary Discussion).

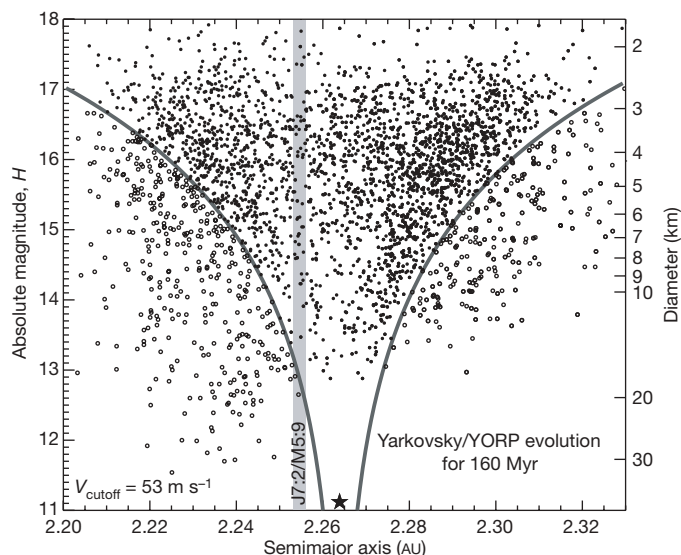


Figure 1 | The orbital and size distribution of the observed Baptistina asteroid family. The family has been projected onto a plane of proper semimajor axis a versus absolute magnitude H . On the right ordinate, we show asteroid diameters for a typical C-type asteroid albedo of 0.04. The central and largest body of the family, C-type asteroid (298) Baptistina¹⁹, has proper semimajor axis $a = 2.264$ AU, eccentricity $e = 0.15$, and sine of inclination $\sin i = 0.10$ (ref. 18). The BAF was identified using the hierarchical clustering method (HCM) applied to the proper orbital element database found in the AstDyS database¹⁸ (see Supplementary Discussion). The HCM locates bodies in the neighbourhood of (298) Baptistina with mutual velocities less than a threshold limit V_{cutoff} . The filled and open circles show 3,042 linked objects with $V_{\text{cutoff}} = 53 \text{ m s}^{-1}$. The family is also noticeably depleted near the adjacent J7:2 and M5:9 resonances²⁰ (grey bar at $a \approx 2.2545$ AU). The two-lobed structure with an evacuated centre is diagnostic of families that have spread in a for an extended time under the influence of Yarkovsky/YORP thermal forces^{21,22}. The dark grey lines that bracket the outside of each lobe represent our best estimate of how far the majority of family members could have spread in ~ 160 Myr. Objects outside these curves, shown as open circles, are assumed to be predominantly interlopers. Most come from the nearby Flora or Vesta families, whose spectroscopic signatures are similar to space-weathered ordinary chondrites (that is, S-type asteroids; Flora family) or basaltic achondrites (HED) meteorites (that is, V-type asteroids; Vesta family)^{19,43,45}. Their number density near a H of ~ 16 , at which the SDSS is sensitive to asteroids, indicates that interlopers between the grey curves only contribute 10–20% to the overall BAF.

To test our BAF identification scheme, we examined the colour properties of BAF members and background asteroids in five photometric bands using data from the Sloan Digital Sky Survey (SDSS)²³. For values near a H of ~ 16 , the number of asteroids with C- or X-type colours between the grey lines in Fig. 1 were found to dominate those with S- or V-type-like colours by at least a factor of 4, values consistent with our estimates (see Supplementary Discussion). Our analysis also showed that all of the asteroids with C- or X-type colours in the innermost region of the main belt near the BAF reside between the grey lines. This provides support for the idea that (298) Baptistina and our predicted BAF members came from the same disruption event.

Size distribution and parent body size

An intriguing aspect of Fig. 1 is the apparent deficiency of BAF members found close to the J7:2/M5:9 relative to the population found near its 'mirror image' location at ~ 2.27 AU, with the centre of symmetry defined as the semimajor axis of (298) Baptistina. Numerical simulations indicate that bodies in the J7:2/M5:9 can have their eccentricities pumped up to Mars-crossing orbits over timescales as short as a few Myr (ref. 20). We infer that an unknown fraction of the BAF has escaped the main belt and entered the terrestrial planet region since the family-forming event took place. To quantify how many kilometre-sized and larger fragments have been lost over time, we must estimate the size–frequency distribution (SFD) created by the BAF's formation and how it has changed over the family's lifetime.

Yarkovsky/YORP modelling work indicates that families with two-lobed structures like those in Fig. 1 are essentially symmetric in (a, H) space²². This means that if the J7:2/M5:9 did not exist, the population on the left side of the BAF should reflect that of the right side. Hence, by doubling the population of the right side of the family (Fig. 1), we obtain an estimate of the BAF's original SFD that accounts for the missing objects on the left side, provided that collisional evolution is unimportant. This 'derived SFD' is shown in Fig. 2.

The cumulative power-law index q of our derived SFD between $10 \text{ km} < D < 20 \text{ km}$ (cumulative number $N(>D) \propto D^q$) is -6.5 to -8 , steep enough to produce ~ 300 $D > 10$ km objects. It then bends to $q \approx -2.7$ for $6 \text{ km} < D < 10 \text{ km}$. Using a Monte Carlo code to account for observational and statistical errors in the H values of known BAF members (see Supplementary Discussion), we fit a power law to the distribution of $6 \text{ km} < D < 10 \text{ km}$ objects, a size range where we are confident the population is both observationally complete and has been relatively unaffected by collisional evolution. This power law was then extrapolated down to $D = 1 \text{ km}$. According to our best-fit results, the initial BAF once contained $(1.36 \pm 0.3) \times 10^5$ objects with $D > 1 \text{ km}$.

The size of the Baptistina parent body cannot be directly computed from observations, partly because $D \lesssim 3 \text{ km}$ BAF members are too small to be detected by existing surveys but also because many have been removed by collisional and dynamical processes. To circumvent this problem, we used numerical impact experiments to gain insights into the circumstances that formed the BAF²⁴. Our simulations, created using a smooth particle hydrodynamic (SPH) code coupled to an N -body code, followed projectiles shot into coherent target asteroids over a wide range of projectile/target mass ratios, collision velocities, and impact angles²⁵. The resultant model SFDs were then compared to the largest bodies of the derived SFD described above; these objects have yet to experience significant collisional evolution²⁴. Because the model SFD must explicitly conserve mass down to the code's resolution limit, a reasonable match at the large diameter end of the SFD allows us to estimate how much of the BAF's mass was initially in the form of smaller objects²⁴. Figure 2 shows our most successful run to date. It indicates that the Baptistina parent body had $D \approx 170 \text{ km}$, and that the BAF's initial SFD had 88% of its mass in the form of $D < 10 \text{ km}$ fragments.

Collisional evolution

Using the derived SFD together with the estimated size of the Baptistina parent body, we computed how collisional evolution has

affected the BAF's SFD over time. This was done using CoDDEM, a one-dimensional self-consistent code capable of tracking the collisional evolution and dynamical depletion of both the BAF and main belt SFDs simultaneously^{1,26}. The starting SFD for the BAF was chosen to match the derived SFD in Fig. 2 as well as constraints provided by the steep fresh crater population on nearby asteroid (951) Gaspra²⁷. The total mass represented by the SFD was required to match the estimated mass of the Baptistina parent body. The main belt SFD was assumed to be in a quasi-steady state, where small objects removed by collisions or the Yarkovsky effect are continually replenished by fresh fragments produced by larger breakup events¹.

Our results show that the BAF's SFD quickly grinds itself down to take on the same shape as the background main belt SFD for $D < 5$ km objects (Fig. 3). This explains why small Baptistina fragments do not dominate the inner main belt population today. Among larger objects, we found that 200 Myr after the BAF formation event took place, the number of $D > 1$ km family members had decreased by $\sim 40\%$. Accordingly, unless the BAF is extremely young, the number of km-sized fragments escaping the main belt today via the J7:2/M5:9 must be a factor of ~ 2 lower than the number that escaped immediately after the BAF formation event.

Dynamical evolution

Additional insights into the BAF's age and dynamical history can be gleaned by modelling how the observed family members have evolved from their initial orbits to those in Fig. 1. This was done by numerically

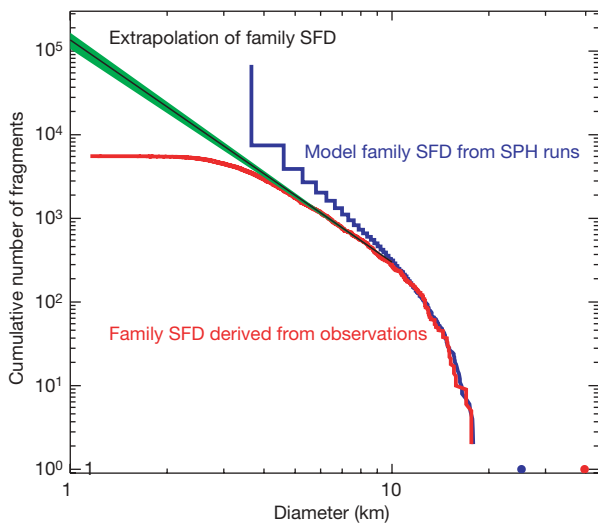


Figure 2 | Estimates of the initial size–frequency distribution of the Baptistina family. The red ‘derived SFD’ comprises (298) Baptistina and twice the family SFD with $a > a_{\text{bap}}$ (4,839 objects in all). The rollover on the left is caused by observational incompleteness. The black curve shows a best fit power law extrapolation from the distribution of $6 \text{ km} < D < 10 \text{ km}$ objects to $D = 1 \text{ km}$, whereas the green shading shows the standard deviation in the fit (see Supplementary Discussion). The blue SFD shows the best fit between the red SFD and model SFDs taken from a suite of 161 SPH/N-body impact simulations²⁵. The target asteroids were $D = 100 \text{ km}$ solid basalt spheres made up of 100,000 individual SPH components. The projectiles were given $D = 10\text{--}46 \text{ km}$, impact speeds of $2.5\text{--}7 \text{ km s}^{-1}$ and impact angles of $15^\circ\text{--}75^\circ$ (that is, nearly head-on to very oblique). The results of each simulation were scaled and compared to the red SFD to estimate the true size of the parent body²⁴. The match between the red and blue curves is very good for $10 \text{ km} < D < 20 \text{ km}$ objects. Although there is a mismatch between the largest remnants of each SFD, which differ in diameter by a factor of 1.6, these objects comprise less than 1% of the parent body's total mass. At $D < 10 \text{ km}$, the SFDs diverge as the model SFD approaches its resolution limit (that is, all model fragments must be in the form of $D > 3.5 \text{ km}$ bodies; this effectively creates an overabundance of $3.5 \text{ km} < D < 10 \text{ km}$ bodies). With considerable parameter space left to explore, our best fit run indicates that the BAF was created by the impact of a $\sim 60\text{-km}$ projectile striking nearly vertical to the surface of a $D \approx 170 \text{ km}$ target body at 3 km s^{-1} .

tracking the simultaneous dynamical and spin vector evolution of test asteroids affected by both the Yarkovsky and YORP effects²². Details of our code and model parameters can be found in the Supplementary Discussion. Our test asteroids, which were given the same sizes as observed BAF members (Fig. 1), were assumed to have been ejected from the current orbit of (298) Baptistina with random trajectories and velocities $V = V_0(D_0/D)$, with $D_0 = 5 \text{ km}$, D the diameter of our test asteroids in km, and V_0 a solved-for velocity parameter in our code. From this initial orbital distribution, the test asteroids were allowed to drift in a according to an established formulation of Yarkovsky/YORP evolution. The bulk density of our test asteroids was set to 1.3 g cm^{-3} , the average bulk density for C-type asteroids²⁸. The goal of our runs was to reproduce the characteristic signature of the BAF in (a, H) , with variables being time since the family-forming event, V_0 , and a parameter C that controls the strength of the YORP effect.

The best fit between our model population and the observed BAF yields a formation age of 160^{+30}_{-20} Myr and characteristic ejecta velocity dispersion $V_0 = 40 \pm 10 \text{ m s}^{-1}$. This makes the BAF the youngest family of its size in the innermost region of the main belt. The timing of the BAF breakup is also interesting, in that it raises the possibility that the Baptistina family-forming event could have influenced the terrestrial planet impactor flux over the Cretaceous period (65–145 Myr ago) and beyond. This would have been accomplished by large BAF members being directly injected and/or driven by the

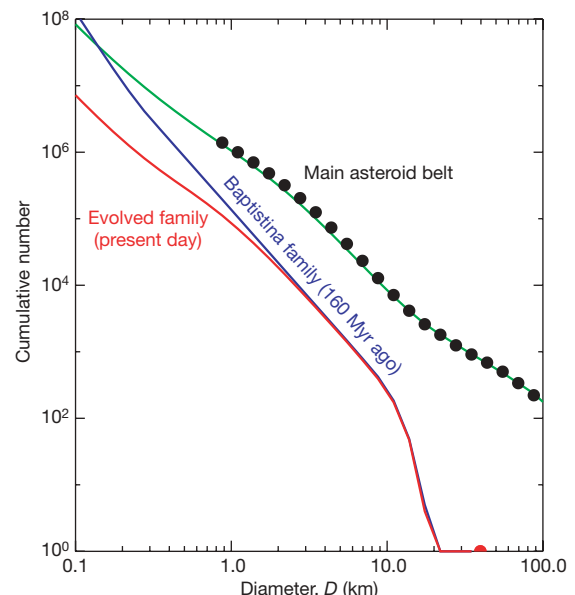


Figure 3 | Collisional evolution of the Baptistina family's size distribution. Using the code CoDDEM^{1,26}, we tracked the evolution of the BAF and main belt SFDs, assuming the objects in each population had bulk densities of 1.3 and 2.7 g cm^{-3} , respectively²⁸. The main belt SFD, asteroid disruption law, and fragment SFDs produced by each individual breakup event are described in ref. 1. The filled circles represent the main belt SFD derived from observations, whereas the green curve is our model main belt SFD. We determined that the intrinsic collision probability (P_i) of Baptistina fragments with one another and with main belt asteroids was 18×10^{-18} and $2.8 \times 10^{-18} \text{ km}^{-2} \text{ yr}^{-1}$, respectively, whereas the impact velocities V_{imp} were 3.9 and 5 km s^{-1} , respectively⁵⁰. The SFDs were tracked for 200 Myr. The figure shows the evolution of the BAF's SFD, assuming that the family forming event took place 160 Myr ago (blue curve). We see that the shape of the BAF's evolved SFD mimics that of the background main belt population for $D < 5 \text{ km}$ objects (red curve). This is because smaller objects are eliminated faster than they can be replenished by disruption events among bigger objects. Conversely, $D > 5 \text{ km}$ objects are harder to disrupt, making them relatively immune to collisional evolution over the timescale of our simulation. Overall, we find the population of $D > 1 \text{ km}$ fragments roughly decreases by 10% over 10 Myr, 20% over 40 Myr, 30% over 100 Myr and 40% over 200 Myr (see Supplementary Discussion).

Yarkovsky effect into the nearby J7:2/M5:9, which is capable of pumping up their eccentricities to planet-crossing values²⁰. Although most BAF escapees would ultimately be eliminated by hitting the Sun or being ejected out of the inner Solar System by an encounter with Jupiter, a small fraction would have gone on to strike the Earth or other planets^{2,15}.

The length and severity of an asteroid shower from the BAF is a function of the BAF's SFD, the likelihood of BAF members reaching the J7:2/M5:9, and the efficiency of the J7:2/M5:9 at producing planetary impactors. To determine the fraction of BAF members pushed out of the main belt by the J7:2/M5:9, we created a model of the initial orbital distribution of the family immediately after the breakup event. Here we took the largest 800 BAF objects with $a > a_{\text{bap}}$ found in Fig. 1 and gave them starting values (a_{start}) consistent with the BAF's initial ejection velocity distribution; $a_{\text{bap}} + (a - a_{\text{bap}})/2$ and $a_{\text{bap}} - (a - a_{\text{bap}})/2$. Next, we tracked the dynamical evolution of test family members using the symplectic integration code SWIFT-RMVS3 (ref. 29) modified to accommodate Yarkovsky thermal forces³⁰. The bodies were assigned sizes of $D = 1, 5$ and 10 km, bulk densities of 1.3 g cm^{-3} (ref. 28), spin periods of 6 ± 2 h (ref. 31), random spin axis orientations, and a thermal inertia of $100 \text{ J m}^{-2} \text{ s}^{-0.5} \text{ K}^{-1}$ (ref. 32). We tracked 1,600 bodies with $D = 1$ km and 900 bodies with $D = 5$ and 10 km. The planets Venus through to Neptune were included in our integrations. See Supplementary Discussion for example runs.

Overall, about 20% of our $D = 5$ and 10 km model asteroids reached the J7:2/M5:9 and escaped the main belt over 160 Myr (see Fig. 4 legend). For our $D = 1$ km bodies, we scaled our raw integration results to account for the effects of YORP; over 10–20 Myr timescales, YORP can spin up a km-sized body to the point that it sheds mass, or spin it down to the point that it readily undergoes a spin axis reorientation event³³ (see also ref. 21). We estimate that these so-called YORP cycles slow the nominal Yarkovsky drift rates of $D = 1$ km bodies by a factor of ~ 3 or so, such that only 13% escaped after 160 Myr.

These runs were also used to determine how many BAF members were in the NEO population today. By tracking the number of model asteroids in the NEO population at 160 Myr of simulation time and

scaling those numbers to account both for YORP cycles (for example, for $D > 1$ km objects, we reduced the population by a factor of 3) and the collisional evolution results described in Fig. 3 (for example, for $D > 1$ km objects, we reduced the population by $\sim 40\%$), we estimate that the current representation of $D > 1$ km BAF members in the NEO population is $\sim 0.18\%$ that of the initial population. Hence, if the BAF initially had $(1.36 \pm 0.3) \times 10^5$ objects of this size (Fig. 2), the current number of km-sized BAF objects in the NEO population today should be 240 ± 50 . For comparison, there are $\sim 1,100$ km-sized NEOs with $a < 7.4$ AU, with half being dark C- or X-type asteroids or dormant Jupiter-family comets^{11,34–36}. This implies that of the NEOs with $D > 1$ km, the BAF may be responsible for 40% of all C- and X-types and 20% of the entire population.

Impact flux on terrestrial planets

To compute the impact rate of BAF members on the terrestrial planets, we numerically integrated 9,024 test bodies placed inside the J7:2/M5:9. Our runs again used SWIFT-RMVS3 (ref. 29) but did not include the Yarkovsky effect because of its limited importance for planet-crossing asteroids. Tracking their evolution throughout the inner Solar System, we found that 1.7% hit Earth over 200 Myr of evolution (see Supplementary Discussion).

Figure 4 shows the expected impact rate distribution of BAF members on Venus, Earth and Mars for $D > 1$ km, $D > 5$ km and $D > 10$ km asteroids. A Monte Carlo code was used to combine the number of BAF objects at time t after the family-forming event with two probability distributions, one describing the likelihood that BAF objects will become trapped in the J7:2/M5:9 at time t and the other describing the likelihood that objects in the J7:2/M5:9 will hit a planet at time t . For Earth impacts, the BAF asteroid shower peaked at $t \approx 40$ Myr and then slowly decayed to the present day. This peak is consistent with an inferred change in the terrestrial impactor flux that occurred 100–120 Myr ago (see, for example, ref. 4). At this time, the number of km-sized BAF asteroids in NEO space was ~ 3 times its current value; this implies that the total NEO population was 1.4 times its present-day size, with $\sim 65\%$ being C- or X-type asteroids.

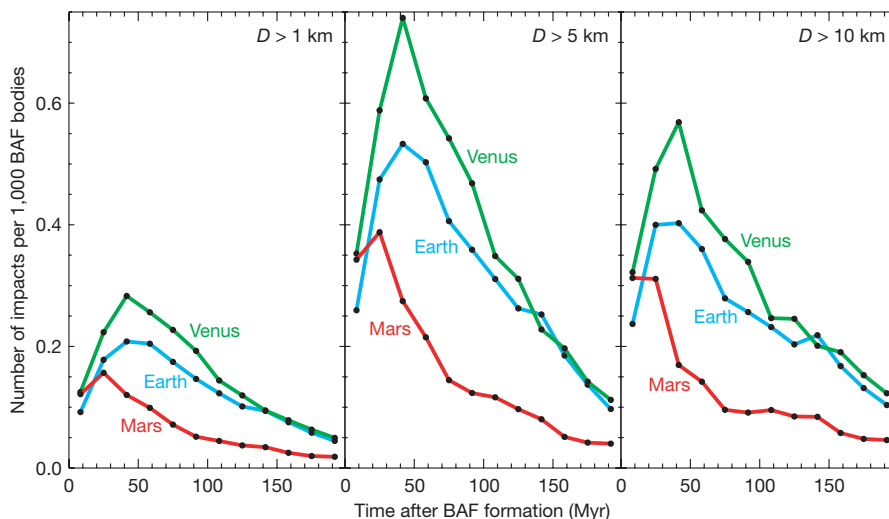


Figure 4 | The impact rate of Baptista fragments on Venus, Earth and Mars. For reference, the ordinate values were normalized to be the number of impacts per 1,000 BAF objects, whereas the abscissa is time after the Baptista family-formation event. This plot was created by combining results from two different numerical simulations within a Monte Carlo code (see Supplementary Discussion). In the first simulation, we created a model BAF and tracked the time needed for test asteroids with $D = 1, 5$ and 10 km to become trapped in the J7:2/M5:9. Scaling for the YORP effect, we found that 13%, 23% and 19%, did this, respectively, over 200 Myr of evolution. The $D > 1$ km value was then further scaled to account for the depletion of these objects by collisional evolution as a function of time (Fig. 3). For the second simulation, we numerically integrated test bodies placed inside the

J7:2/M5:9 and determined both the fraction that struck Venus, Earth and Mars, and the times of these impacts. These runs included perturbations from the planets Venus through to Neptune but excluded the Yarkovsky effect. We found that 2.1%, 1.7% and 0.9% hit Venus, Earth and Mars over 200 Myr of evolution. Using our Monte Carlo code, we randomly added times together from both simulations and then tabulated the results over 500,000 simulations. Assuming that the BAF is 160 Myr old, the number of $D > 1$ km, $D > 5$ km and $D > 10$ km impacts on Earth over this time are 200 ± 60 , 6 ± 2 and 1 ± 1 , respectively, whereas those from the background are 260 ± 20 , 3 ± 2 and 0.5 ± 0.7 , respectively. Hence, the Baptista asteroid shower increased the impact flux on the Earth and Moon by a factor of 2–3 for multi-kilometre projectiles.

When this information is combined with the BAF escape rates provided above and the evolved SFD shown in Fig. 3, we get impact rates that indicate the Earth should have been hit over the past 160 Myr by 200 ± 60 objects with $D > 1$ km, 6 ± 2 objects with $D > 5$ km, and 1 ± 1 objects with $D > 10$ km (see Supplementary Discussion). For the latter value, assuming Poisson statistics, the formal probability that one or more $D > 10$ km objects has hit the Earth over the past 160 Myr is 60%. The relationship between the largest BAF impactor and the K/T event is discussed below.

Numerical calculations indicate that $D > 1$ km asteroids currently strike the Earth, on average, every 0.5 Myr (refs 11, 35, 36). If we remove the estimated BAF contribution, this value changes to ≥ 0.63 Myr. Inserting these rates into a Monte Carlo code, we find that over the past 160 Myr, km-sized BAF members have struck the Earth 200 ± 60 times whereas those from the background population have hit 260 ± 20 times (see also Fig. 4 legend). These values are in excellent agreement with the approximate factor of 2 increase in the km-sized impactor flux inferred from terrestrial and lunar craters and the lunar glass spherule data^{3–6,8,9}. It also suggests that the majority of craters formed ~ 100 – 120 Myr ago were made by C- and X-type projectiles, a prediction that should be testable.

Origin of the K/T impactor

The K/T mass extinction event, which was by far the largest of the Mesozoic and Cenozoic eras (that is, the last 250 Myr), has been strongly linked to the formation of the 180-km-wide Chicxulub crater that formed 65 Myr ago^{37,38}. It was produced by the impact of a ~ 10 -km projectile (see refs 37 and 39, also <http://www.lpl.arizona.edu/tekton/crater.html>). The two possible sources for this event are the BAF asteroid shower and a background NEO population that includes comets. Here we estimate the relative likelihood that either produced the Chicxulub crater.

First it is useful to describe what we know of the Chicxulub impactor. Chromium found in sediment samples taken from different K/T boundary sites^{40,41}, as well as a meteorite found in K/T boundary sediments from the North Pacific Ocean⁴², suggest the impactor was a CM2-type carbonaceous chondrite. This classification is consistent with the C- and X-type taxonomy of the BAF and rules out the possibility that the K/T impactor came from an S- or V-type asteroid⁴³. Hence, if the K/T impactor came from the background NEO population, it had to come out of the relatively small fraction that had C-type, X-type or comet taxonomy 65 Myr ago. As described above, this would be equivalent to $50\% - 20\% \approx 30\%$ of the present-day population. As a check on this value, we examined all of the $D \geq 10$ km NEOs with known taxonomic types; according to our model, nearly all should now be background objects. We found 6 of 7 (86%) have S-type taxonomy, consistent with our estimate that $>70\%$ should be this way.

Next, we examined the impact flux from each source. The terrestrial impact rate of $D > 10$ km projectiles from the BAF is ~ 1 over the past 160 Myr. The frequency of comparable impacts from the background NEO population is more difficult to calculate for several reasons: (1) the current orbital and size distribution of large NEOs is not necessarily representative of time-averaged conditions^{2–6}, (2) no $D > 10$ km impactors are currently on Earth-crossing orbits¹⁸, and (3) the population of large terrestrial craters is incomplete and suffers from selection effects (for example, removal of craters by erosion, and observing biases)^{3,4}.

To avoid these problems, we computed the current escape rate of $D > 10$ km bodies from the inner main belt and their estimated terrestrial impact rate. This source is thought to dominate the large body impactor flux from the background NEO population with $a < 7.4$ AU, so the impact rates from several other background sources (for example, outer main belt, active and dormant Jupiter-family comets) can be folded into this value^{2,11}. According to our model results, the BAF contribution to the $D > 10$ km flux is minimal at present, such that the large object flux is arguably more likely to represent

time-averaged conditions over the past several hundred Myr than existing NEOs. Numerical results² indicate that one $D > 10$ km body escapes the inner main belt every ~ 4 Myr and that 1.25% of them strike the Earth⁴⁴. This translates into an approximate impact rate of one per 350 Myr. If we then assume that $<30\%$ of the background were C- and X-type asteroids or Jupiter family comets 65 Myr ago, and only 40% of those objects had CM-like compositions, estimates that are consistent with present-day meteorite fall statistics⁴⁵, the impact flux drops to one per 3,500 Myr. A comparable value was found when we examined the possibility that the K/T impactor came from nearly isotropic comets (see Supplementary Discussion). Combining these rates, we predict that primitive K/T-like projectiles from the background population strike the Earth once per 1,800–2,600 Myr.

Using these impact rates as input for a Monte Carlo code, we find there is a $\lesssim 10\%$ chance that the K/T impactor was derived from the background and a $\geq 90\%$ chance it came from the BAF. Accordingly, we predict that the most likely cause of the K/T mass extinction event was a collision between the Earth and a large fragment from the Baptistina asteroid shower.

Support for a connection between CM meteorites and the BAF can be found by examining what is known about the meteorite delivery process. Collision and dynamical modelling work on asteroid families tell us that large families in the innermost region of the main belt, which produce numerous meteoroids via a collisional cascade and have access to the most efficient dynamical pathways to reach Earth, are expected to dominate our meteorite fall statistics^{26,44}. Considering that the BAF is the only prominent C- or X-type family in this region, we predict it should be the source of the largest class of carbonaceous chondrite falls, which happens to be that of the CM meteorites⁴⁵. Accordingly, the CM meteorite and $D \approx 170$ km Baptistina parent bodies are likely to be one and the same.

Additional implications

The lunar crater Tycho is something of a statistical anomaly when one considers its large size (85 km) and relatively young age (109 ± 4 Myr; see ref. 46). Calculations suggest that Tycho was created by the impact of a $D > 4$ km projectile³⁹. Using our work, we estimate that 0.6 BAF members of this size have hit the Moon over the past 160 Myr, whereas the impact rate from the background population is one per 570 Myr (ref. 2). The contribution from nearly isotropic comets is negligible. Because there is no compositional information on the Tycho projectile, we cannot pare these numbers further. Incorporating them into a Monte Carlo code, we find there is a $\sim 70\%$ chance that the projectile that created Tycho was from the BAF rather than the background population. The fact that Tycho formed near the peak of the Baptistina asteroid shower is also suggestive of a link between the two (Fig. 4).

Similar techniques were used to investigate the formation history of the largest craters on Venus: Mead (269 km), Isabella (176 km), Meitner (151 km) and Klenova (142 km)⁴⁷. Numerical simulations show that these craters formed over the past 730 Myr (ref. 48) from roughly K/T-sized projectiles striking the venusian surface³⁹. Estimates of the background impactor flux indicate that projectiles this size strike Venus and Earth at nearly the same rate (one per ~ 350 Myr; ref. 2). Using these data as well as information from Figs 2 and 4, we found an 80% probability that at least one of these craters was produced by the Baptistina asteroid shower (see Supplementary Discussion).

Probing the martian impactor flux, we estimate that approximately 110 $D > 1$ km BAF fragments have struck Mars over the past 160 Myr. For the background population over the same size range, the interval between impacts is roughly 1.3 Myr (ref. 2). This means that the impact rate of $D > 1$ km bodies on Mars has nearly doubled over the past 160 Myr, with most impactors striking within a few tens of Myr after the Baptistina parent body disrupted (Fig. 4). It will be interesting to see how further studies of the Baptistina asteroid shower affect our understanding of recent martian chronology.

The BAF also has some surprising implications for asteroids in the main belt itself. (951) Gaspra, a $19 \times 12 \times 11$ km S-type asteroid in the Flora family, has a fresh, non-saturated population of $D < 0.6$ km craters whose SFD is far steeper ($q = -3.3 \pm 0.3$; ref. 27) than expectations based on collisional models of the main belt production population (for example, $q \approx -2.5$; ref. 1). We find that the majority of these craters may have been produced by an intense barrage of sub-100-m fragments tied to the Baptistina family-forming event²⁷. If true, the signature of this bombardment should also exist on other asteroids that once had, or still have, Baptistina-like orbits.

The interval between $D > 100$ km disruption events across the main belt is short enough (~ 200 Myr; refs 1, 24) that other asteroid showers should have occurred in the past¹⁵. The Flora family, which was created 470 Myr ago by the disruption of a $D > 200$ km S-type asteroid residing near $a \approx 2.2$ AU (refs 17, 24, 49), seems to be the best candidate to have produced a relatively recent Baptistina-like asteroid shower. The family's age has been precisely determined by linking its ejecta to the existence of tiny L-chondrite meteorites found within the limestone walls of a Swedish quarry^{16,17}. Preliminary work suggests that the Flora family lost a significant fraction of its initial population of $D > 1$ km asteroids to Mars-crossing orbits (see, for example, ref. 49). If so, this putative shower may explain the abundance of ~ 200 – 500 -Myr-old impact-derived glass spherules found in lunar soils⁹ as well as the increased number of lunar craters formed over these same ages⁸.

Received 11 April; accepted 22 June 2007.

1. Bottke, W. F. *et al.* Linking the collisional history of the main asteroid belt to its dynamical excitation and depletion. *Icarus* **179**, 63–94 (2005).
2. Bottke, W. F. *et al.* Debaised orbital and absolute magnitude distribution of the near-Earth objects. *Icarus* **156**, 399–433 (2002).
3. Shoemaker, E. M. Impact cratering through geologic time. *J. R. Astron. Soc. Can.* **92**, 297–309 (1998).
4. Grieve, R. A. F. & Shoemaker, E. M. in *Hazards Due to Comets and Asteroids* (eds Gehrels, T. & Matthews, M. S.) 417–462 (Univ. Arizona Press, Tucson, 1994).
5. McEwen, A. S., Moore, J. M. & Shoemaker, E. M. The Phanerozoic impact cratering rate: Evidence from the farside of the Moon. *J. Geophys. Res.* **102**, 9231–9242 (1997).
6. Grier, J. A. *et al.* Optical maturity of ejecta from large rayed lunar craters. *J. Geophys. Res.* **106**, 32847–32862 (2001).
7. Ward, S. N. & Day, S. Terrestrial crater counts: Evidence for a four-fold increase in bolide flux at 125 Ma. ([http://es.uscc.edu/~ward/papers/crater-counts\(v1.8\).pdf](http://es.uscc.edu/~ward/papers/crater-counts(v1.8).pdf)) (2007).
8. Baldwin, R. B. Relative and absolute ages of individual craters and the rate of infalls on the moon in the post-Imbrium period. *Icarus* **61**, 63–91 (1985).
9. Levine, J., Becker, T. A., Muller, R. A. & Renne, P. R. ⁴⁰Ar/³⁹Ar dating of Apollo 12 impact spherules. *Geophys. Res. Lett.* **32**, L15201, doi:10.1029/2005GL022874 (2005).
10. Dones, L. *et al.* in *Comets II* (eds Festou, M. C. *et al.*) 153–174 (Univ. Arizona Press, Tucson, 2004).
11. Stokes, G. *et al.* A study to determine the feasibility of extending the search for near Earth objects to smaller limiting magnitudes. (neo.jpl.nasa.gov/neo/report.html) (2003).
12. Levison, H. *et al.* The mass disruption of Oort cloud comets. *Science* **296**, 2212–2215 (2002).
13. Tagle, R. & Claeys, P. Comet or asteroid shower in the Late Eocene? *Science* **305**, 492 (2004).
14. Maier, W. D. *et al.* Discovery of a 25-cm asteroid clast in the giant Morokweng impact crater, South Africa. *Nature* **441**, 202–206 (2006).
15. Zappalà, V., Cellino, A., Gladman, B. J., Manley, S. & Migliorini, F. Asteroid showers on Earth after family breakup events. *Icarus* **134**, 176–179 (1998).
16. Schmitz, B., Håggström, T. & Tassinari, M. Sediment-dispersed extraterrestrial chromite traces a major asteroid disruption event. *Science* **300**, 961–964 (2003).
17. Nesvorný, D., Vokrouhlický, D., Bottke, W. F., Gladman, B. J. & Håggström, T. Express delivery of fossil meteorites from the inner asteroid belt to Sweden. *Icarus* **188**, 400–413 (2007).
18. Knežević, Z. & Milani, A. Proper element catalogs and asteroid families. *Astron. Astrophys.* **403**, 1165–1173 (2003).
19. Mothé-Diniz, T., Roig, F. & Carvano, J. M. Reanalysis of asteroid families structure through visible spectroscopy. *Icarus* **174**, 54–80 (2005).
20. Morbidelli, A. & Nesvorný, D. Numerous weak resonances drive asteroids toward terrestrial planets orbits. *Icarus* **139**, 295–308 (1999).
21. Bottke, W. F., Vokrouhlický, D., Rubincam, D. P. & Nesvorný, D. The Yarkovsky and YORP effects: Implications for asteroid dynamics. *Annu. Rev. Earth Planet. Sci.* **34**, 157–191 (2006).
22. Vokrouhlický, D., Brož, M., Bottke, W. F., Nesvorný, D. & Morbidelli, A. Yarkovsky/YORP chronology of asteroid families. *Icarus* **182**, 111–142 (2006).
23. Ivezić, Ž. *et al.* Color confirmation of asteroid families. *Astron. J.* **124**, 2943–2948 (2002).
24. Durda, D. D. *et al.* Size–frequency distributions of fragments from SPH/N-body simulations of asteroid impacts: Comparison with observed asteroid families. *Icarus* **186**, 498–516 (2007).
25. Durda, D. D. *et al.* The formation of asteroid satellites in catastrophic impacts: Results from numerical simulations. *Icarus* **167**, 382–396 (2004).
26. Bottke, W. F. *et al.* in *Dynamics of Populations of Planetary Systems* (eds Knežević, Z. & Milani, A.) 357–376 (Cambridge Univ. Press, Cambridge, UK, 2005).
27. Bottke, W. F., Vokrouhlický, D., Chapman, C. R. & Nesvorný, D. Gaspra's steep crater population was produced by a large recent breakup in the main asteroid belt. *Lunar Planet. Sci. Conf. abstr.* 2165 (2007).
28. Britt, D. T. *et al.* in *Asteroids III* (eds Bottke, W. F. *et al.*) 485–500 (Univ. Arizona Press, Tucson, 2002).
29. Levison, H. F. & Duncan, M. J. The long-term dynamical behavior of short-period comets. *Icarus* **108**, 18–36 (1994).
30. Brož, M. *Yarkovsky Effect and the Dynamics of the Solar System*. PhD thesis, Charles Univ. (2006); (<http://sirrah.troja.mff.cuni.cz/~mira/mp/>) (2006).
31. Pravec, P., Harris, A. W. & Michalowski, T. in *Asteroids III* (eds Bottke, W. F. *et al.*) 113–122 (Univ. Arizona Press, Tucson, 2002).
32. Delbò, M. *et al.* Thermal inertia of near-Earth asteroids and implications for the magnitude of the Yarkovsky effect. *Icarus*. (in the press).
33. Vokrouhlický, D. & Čapek, D. YORP-induced long-term evolution of the spin state of small asteroids and meteoroids. Rubincam's approximation. *Icarus* **159**, 449–467 (2002).
34. Stuart, J. S. & Binzel, R. P. Bias-corrected population, size distribution, and impact hazard for the near-Earth objects. *Icarus* **170**, 295–311 (2004).
35. Morbidelli, A. *et al.* From magnitudes to diameters: The albedo distribution of near Earth objects and the Earth collision hazard. *Icarus* **158**, 329–342 (2002).
36. Binzel, R. P. *et al.* Observed spectral properties of near-Earth objects: results for population distribution, source regions, and space weathering processes. *Icarus* **170**, 259–294 (2004).
37. Alvarez, L. W., Alvarez, W., Asaro, F. & Michel, H. V. Extraterrestrial cause for the Cretaceous Tertiary extinction. *Science* **208**, 1095–1108 (1980).
38. Kring, D. A. The Chicxulub impact event and its environmental consequences at the K/T boundary. *Palaeogeogr. Palaeoclimatol. Palaeoecol.* (in the press).
39. Melosh, H. J. *Impact Cratering: A Geologic Process* (Oxford Univ. Press, New York, 1989).
40. Shukolyukov, A. & Lugmair, G. W. Isotopic evidence for the Cretaceous-Tertiary impactor and its type. *Science* **282**, 927–930 (1998).
41. Trinquier, A., Birck, J.-L. & Allègre, J. C. The nature of the K/T impactor. A ⁵⁴Cr reappraisal. *Earth Planet. Sci. Lett.* **241**, 780–788 (2006).
42. Kyte, F. T. A meteorite from the Cretaceous-Tertiary boundary. *Nature* **396**, 237–239 (1998).
43. Clark, B. E. in *Asteroids III* (eds Bottke, W. F. *et al.*) 585–599 (Univ. Arizona Press, Tucson, 2002).
44. Bottke, W. F. *et al.* Iron meteorites as remnants of planetesimals formed in the terrestrial planet region. *Nature* **439**, 821–824 (2006).
45. Burbine, T. H. *et al.* in *Asteroids III* (eds Bottke, W. F. *et al.*) 653–667 (Univ. Arizona Press, Tucson, 2002).
46. Stöffler, D. & Ryder, G. Stratigraphy and isotope ages of lunar geologic units: Chronological standard for the inner solar system. *Space Sci. Res.* **96**, 9–54 (2001).
47. Herrick, R. R. *et al.* in *Venus II* (eds Bougher, S. W. *et al.*) 1015–1046 (Univ. Arizona Press, Tucson, 1997).
48. Korycansky, D. G. & Zahnle, K. J. Modeling crater populations on Venus and Titan. *Planet. Space Sci.* **53**, 695–710 (2005).
49. Nesvorný, D. *et al.* The Flora family: A case of the dynamically dispersed collisional swarm? *Icarus* **157**, 155–172 (2002).
50. Bottke, W. F. *et al.* Velocity distribution among colliding asteroids. *Icarus* **107**, 255–268 (1994).

Supplementary Information is linked to the online version of the paper at www.nature.com/nature.

Acknowledgements We thank K. Beatty, C. Chapman, L. Dones, D. Durda, B. Enke, D. Kring, F. Kyte, M. Gounelle, R. Grimm, A. Harris, H. Levison, A. Morbidelli, A. Rubin, E. Scott, A. Stern and M. Zolensky for discussions and comments. We also thank G. Williams of the Minor Planet Center for computing revised H values and observational errors for the Baptistina family. The work of W.F.B. and D.N. on this project was supported by NASA's Origins of Solar System, Planetary Geology and Geophysics, and Near-Earth Objects Observations programmes. D.V. was supported by the Grant Agency of the Czech Republic.

Author Information Reprints and permissions information is available at www.nature.com/reprints. The authors declare no competing financial interests. Correspondence and requests for materials should be addressed to W.F.B. (bottk@boulder.swri.edu).